the unprepared mound floor, 5 feet from the northern edge of the excavation. Most of the remaining portion of mound 2 was excavated during the summer of 1966, in an attempt to establish its age. Significant traits uncovered, which identify the site as middle Adena, are the presence of a prepared clay base and a bark-covered extended burial. The few flint artifacts recovered are all from the mound fill, mostly Archaic point types but including one ovate base Adena stemmed point.

Charcoal taken from the mound floor was radiocarbon dated at 280 B.C. ± 140 years (*1*), which accords well with the archeological evidence available from the excavation.

The ear of maize from Daines Mound 2 is a small, ten-rowed ear of "Tropical Flint," still partly enclosed in the inner husk. The ear greatly resembles Tropical Flint maize available from Hopewellian sites in the eastern United States (*2*). The earliest known occurrence of such Hopewellian maize is that from the Newman site, Moultrie County, Illinois, dated at 50 B.C. ± 140 and 80 B.C. ± 140 years (*3*). Reports of maize from Kentucky rock shelters have been dismissed as possible occurrences of Adena maize because the finds have been limited to the upper levels of the sites, which represent later, younger components (*4*).

Dragoo (*5*) observed that as yet no maize had been discovered in unquestionable association with an Adena

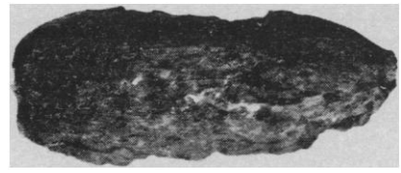

5 cm

Fig. 1. Ear of "Tropical Flint" maize from base of Daines Mound 2, Athens, Athens County, Ohio (Photo courtesy of H. C. Cutler and L. W. Blake).

component. The presence of maize at Daines Mound 2 indicates that maize agriculture was present in the Adena phase, though this unique occurrence allows no conclusions regarding the extent and importance of maize within Adena.

JAMES L. MURPHY
Department of Geology,
Case-Western Reserve University,
Cleveland, Ohio 44106

References and Notes

1. H. R. Crane and J. B. Griffin, *Radiocarbon* **12**, 170 (1970).
2. H. C. Cutler and L. W. Blake, unpublished data.
3. H. R. Crane and J. B. Griffin, *Radiocarbon* **10**, 81 (1968).
4. R. M. Goslin, in *The Adena People—No. 2*, W. S. Webb and R. S. Baby, Eds. (Ohio Historical Society, Columbus, 1957), p. 45.
5. D. W. Dragoo, *Mounds for the Dead: An Analysis of the Adena Culture* (Carnegie Museum, Pittsburgh, 1963), pp. 223–225.
6. I thank Mr. and Mrs. R. Daines for permission to excavate the Daines mounds; Dr. H. Hultgren, his students, and other Ohio University students for help in excavation; and M. Moskal for allowing the maize to be examined by H. Cutler and L. Blake.

3 December 1970

Ribosomal RNA Synthesis and the Multiple, Atypical Nucleoli in Cleaving Embryos

Abstract. *The rate of ribosomal RNA synthesis per nucleus in cleaving sea urchin embryos is similar to the rate at later embryonic stages. The multiple, atypical nucleoli, present in early embryos and usually attributed to decreased ribosomal RNA synthesis, are beginning stages of nucleolar formation. Full nucleolar development requires more time than the brief interphase of the rapidly dividing cells.*

It has been reported that synthesis of ribosomal RNA (rRNA) cannot be detected until the end of blastula stages of sea urchin, amphibian, and certain other embryos; this suggests that rRNA synthesis is decreased or repressed during early stages of development in these embryos (*1*). We have discovered that DNA-like RNA accumulates so much more extensively in early sea urchin embryos than in late embryos that newly synthesized rRNA would not have been detected even if synthesis of rRNA were occurring in early embryos at the rate per nucleus observed in late embryos (*2*). We now report experiments designed to detect and measure the rRNA synthesized during cleavage and to clarify the nature of the atypical nucleoli (*3*) previously thought to be related to a repression of rRNA synthesis during cleavage.

The rate of synthesis of rRNA was measured during cleavage in *Strongylocentrotus purpuratus* embryos that had been incubated at 18°C from 2 to 12 hours of development [from first cleavage until the beginning of blastula stage (*2*)] with either [^{32}P]phosphate or [^{3}H]adenosine to label their RNA. The ^{3}H- and ^{32}P-labeled RNA's were purified by phenol extraction (*2*) and centrifuged separately on sucrose gradients (Fig. 1). The radioactive RNA had the expected heterogeneous size distribution, with no peaks of radioactivity associated with the optical density peaks of 18*S* and 28*S* ribosomal RNA. The radioactive RNA from the embryos incubated with [^{3}H]adenosine was used to measure the absolute amounts of RNA synthesized because the specific activity of the ribose adenosine triphosphate (ATP) precursor pool could be determined by the very sensitive luciferase assay (*2*, *4*). The RNA labeled with ^{32}P was processed to purify the rRNA because the distinctive base composition of rRNA could be used to determine the amount of radioactive rRNA in the purified preparation.

The average specific radioactivity of the ribose ATP pool during the period of incubation with [^{3}H]adenosine was measured as described (*2*, *4*) and was 1.60×10^{14} count/min per mole of ATP. If rRNA was synthesized at 8×10^{-16} g/hour per nucleus, the rate measured in pluteus (*2*), the amount of ^{3}H radioactivity that would have been incorporated into 28*S* ribosomal RNA could be calculated from this specific activity of the ATP. This amount of ^{3}H is plotted as a small hatched area in Fig. 1 and would account for 6 percent of the radioactivity in the fractions at the peak of 28*S* rRNA optical density. This much radioactivity in the rRNA of the embryos labeled with ^{32}P would amount to 94 count/min of ^{32}P per microgram of total rRNA.

The amount of ^{32}P really incorporated into 28*S* rRNA was measured by purifying the small amount of radioactive rRNA from the radioactive DNA-like RNA in the peak of 28*S* ribosomal rRNA. A methylated albumin kieselguhr (MAK) column eluted with a very shallow salt gradient separates rRNA from DNA-like RNA if the RNA's are approximately the same size (*2*). The RNA from a single fraction of a sucrose gradient is similar in size. When run on the MAK column, most of the radioactivity in the 28*S* RNA fractions from the sucrose gradient eluted after

the optical density of bulk rRNA and had a DNA-like base composition, 40 to 43 percent being guanine plus cytosine (G + C) (Fig. 2). A very small peak of radioactivity eluted with the bulk rRNA. The base composition of this peak was 57 percent G + C, as would be expected if this radioactive RNA contained a high percentage of 28*S* rRNA, which has a 61 percent G + C base content (*2*). The exact amount of radioactivity in rRNA can be calculated because the RNA in these column fractions is composed of mainly two classes of RNA (*2*), one DNA-like RNA with 43 percent G + C and the other rRNA with 61 percent G + C. A 57 percent G + C base content indicates that 14/18 of the radioactivity associated with the peak of rRNA (fractions 17 to 21) is in rRNA. This amount of radioactivity is equal to 73 count/min of ^{32}P per microgram of rRNA, an amount very similar to that predicted if rRNA were synthesized in cleaving embryos at the same rate as in pluteus embryos.

This amount of radioactivity in rRNA was confirmed by two other estimates. The same calculation of the ^{32}P radioactivity in rRNA was made for the RNA in other fractions eluting from the MAK column in Fig. 2 at overlapping positions between the peaks of rRNA and DNA-like RNA. Radioactive RNA in fractions 25 and 26 has a 50 percent G + C base content and a calculated 72 count/min per microgram of rRNA. Fractions 31 and 32 have 47 percent G + C and a calculated 94 count/min per microgram of rRNA. Some of the rRNA from the peak of rRNA (fractions 17 to 21) from the MAK column was further purified by recentrifugation on a sucrose gradient. The base composition of the peak of radioactivity associated with the rRNA was 58 percent G + C, and the radioactivity in rRNA was 66 count/min per microgram. These values agree with the 73 count/min per microgram calculated for the peak of rRNA from the MAK column.

Previous suggestions that rRNA synthesis was repressed during cleavage were based on a failure to detect incorporation of RNA precursors into peaks of RNA with a high G + C base content, sedimenting with the peaks of rRNA. Quantitative measurements showed that such results were not sufficient basis to conclude that rRNA synthesis is reduced at these times (*2*). Our data show that RNA having the characteristics of rRNA is synthesized in cleaving cells at about 75 to 80 percent of the rate of rRNA synthesis during the pluteus stage. The slightly reduced synthesis which our data suggest in cleaving cells may not be significantly different from the rate of rRNA synthesis in pluteus cells, but it would not be surprising if rRNA synthesis were slightly depressed during cleavage since the cells are in mitosis about 25 percent of the time.

Since rRNA synthesis is not significantly reduced during cleavage, why are the nucleoli, the sites of rRNA synthesis not fully developed in early embryos (*3*)? These nucleoli do not stain heavily for RNA, nor do they have an extensive granular element typical of normal nucleoli. The descriptions of nucleoli during early development suggested that there might be a correlation between the atypical nucleolar structure and the rapid rate of cell division. We wondered if these incomplete nucleoli were immature

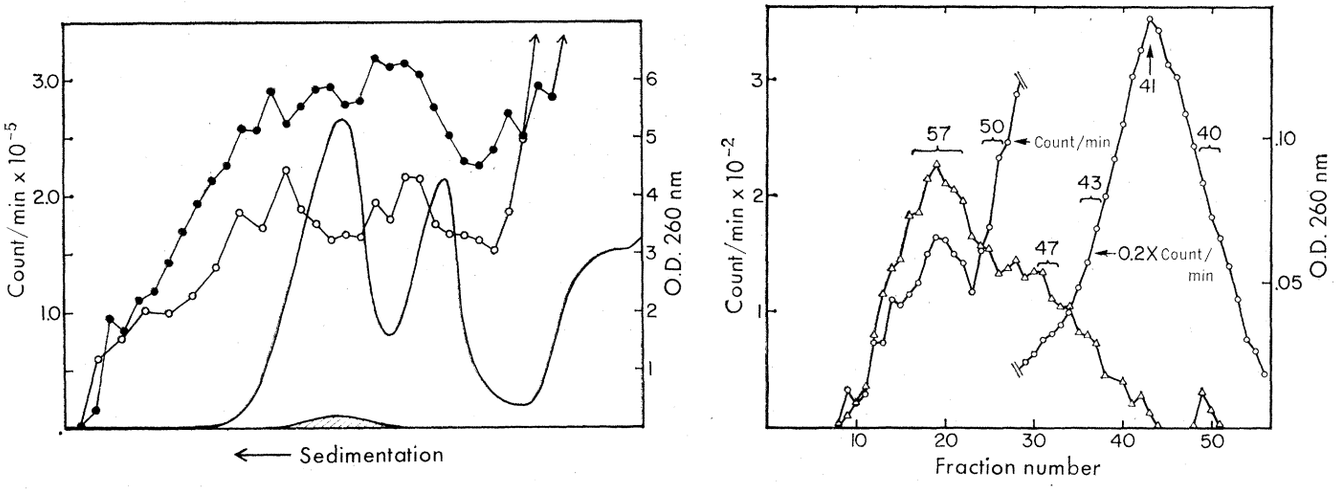

Fig. 1 (left). Sucrose gradient centrifugation of RNA from cleaving sea urchin embryos. Embryos (1×10^6) were incubated at 18°C from 2 to 12 hours of development with either [8-^{3}H]adenosine (3.5 μc/ml; 28 c/mmole) or $^{32}PO_4$ (50 μc/ml; carrier free). RNA was extracted with phenol (*2*) and sedimented separately on 38 ml, linear sucrose gradients (15 to 35 percent) in SDS buffer (0.5 percent sodium dodecyl sulfate, 0.1*M* NaCl, 0.001*M* EDTA, 0.01*M* tris, *p*H 7.5) at 26,000 rev/min for 12 hours (Spinco SW27 rotor) at 30°C. The absorbance at 260 nm (solid line, which was identical in the two gradients) and trichloroacetic acid (5 percent) precipitable radioactivity (●, ^{32}P embryos; ○, ^3H embryos) were determined in the gradients (*2*). The specific activity in the ribose ATP precursor pool was measured in the embryos labeled with [^{3}H]adenosine at 0.3, 1.5, and 12 hours and was constant at 1.6×10^{14} count/min per mole of ATP during this period. The nuclei were counted, and an average of 105 per embryo were present during the incubation period. The ^3H radioactivity expected in rRNA if synthesis were occurring at the rate per nucleus observed in pluteus (*2*) was calculated and is shown by the small hatched area under the peak of 28*S* rRNA. Fig. 2 (right). Column chromatography on MAK of 28*S* RNA. Two fractions (18 and 19) from the 28*S* ribosomal RNA peak of the ^{32}P-labeled RNA on the sucrose gradients illustrated in Fig. 1 were chromatographed with 0.8*M* to 1.1*M* NaCl gradient on a MAK column (*2*). Fractions (5 ml) were collected, and rRNA was monitored by absorbance at 260 nm (△) and the radioactivity of the fraction precipitated by TCA (○) was determined for each fraction (*2*). The scale for radioactivity was reduced fivefold at fraction 28. The numbers over selected fractions indicate their G + C content. Base composition of the fractions was determined after an 18-hour hydrolysis at 37°C in 0.3*N* NaOH. The nucleotides were desalted with charcoal (*2*) and chromatographed on 60-cm Whatman No. 1 paper saturated with Na_2SO_4 (dipped in 20 percent Na_2SO_4 and dried). The spots were separated by descending chromatography over 30 hours. During this time 80 percent ethanol was allowed to drop from the end of the paper. The four spots of nucleotides were cut from the paper and the radioactivity (count/min) was determined.

nucleoli that did not develop fully during the short interphase periods characteristic of cleaving embryos. The fact that each cell contained several nucleoli during early stages, supported this interpretation. In the cells of many organisms, the nucleolus reappears after mitosis as a number of small nucleolar blobs that finally give rise to the definitive nucleolus (*5*). This maturation process probably would not have time to go to completion during the short interphase period.

In order to study the nucleolar cycle during cleavage we found a population of *Lytechinus pictus* that produced especially clear eggs suitable for phase microscopy and began to observe the nucleoli as the cells cleaved. Certain batches of eggs proved superior for observation because their nucleoli were much larger. It soon became obvious that gametes from certain individuals tended to produce embryos with larger nucleoli. The effects of sperm and egg appeared to be additive. By selecting appropriate males and females, we were able to produce different batches of embryos with nucleoli ranging from a barely visible diameter of less than 1 μm at the two-cell stage to a maximum diameter of 6 μm at this stage. In embryos of both types, nucleoli tended to become smaller as the cells and nuclei became smaller during cleavage.

Using sperm and eggs producing embryos with large nucleoli, we followed the development of nucleoli during the interphases of the first few cell divisions of cleavage. Just before a cell entered mitosis, one to four nucleoli were usually visible (Fig. 3a). As soon as the nuclear membrane broke down, these nucleoli dissolved and about eight to ten small blobs appeared when the nucleus reformed after mitosis (Fig. 3b). These blobs grew and could be observed to fuse together (Fig. 3c); and by the end of the 15 minutes of interphase they reached an easily visible size (Fig. 3d), although they still were not as dense or prominent as typical nucleoli at pluteus stages. It appeared as if the nucleoli would have continued to develop if entry into mitosis had not in-

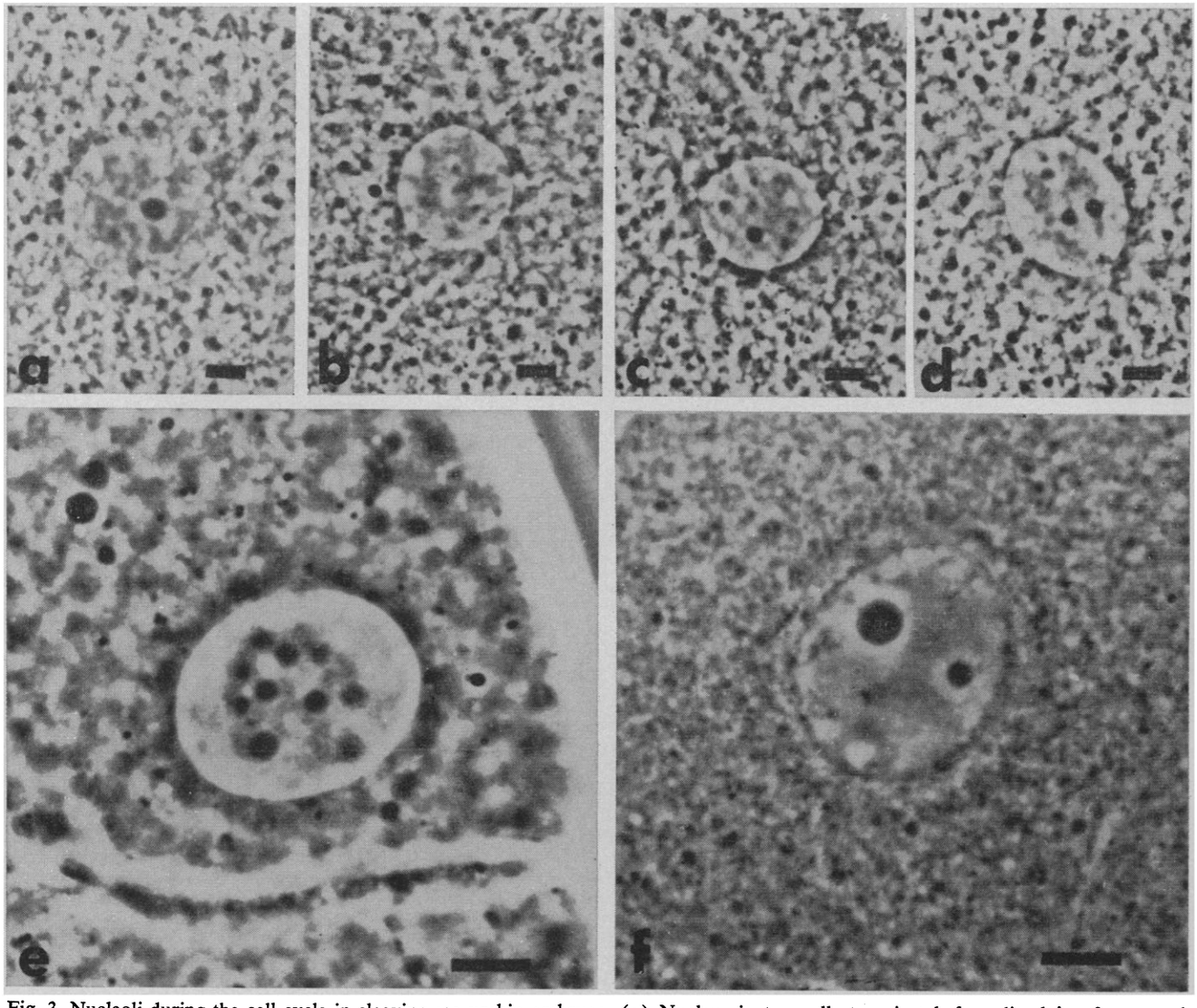

Fig. 3. Nucleoli during the cell cycle in cleaving sea urchin embryos. (a) Nucleus in two-cell stage just before dissolving for second cleavage, one large nucleolus. (b) Newly formed nucleus after second cleavage, many small "nuclear blobs." (c) Five minutes after nucleus reformed. Some nucleolar blobs have fused. (d) Nucleus just before entry into third cleavage, two large nucleoli. (e) Multiple large nucleoli formed when cell division was inhibited with FUdR. (f) Nucleoli formed when nucleolar fusion continues after inhibition of cell division with FUdR. Scales indicate 5 μm.

tervened. The nucleolar cycle in embryos with small nucleoli appeared much the same, except that the nucleoli were generally smaller and tended to fuse much less rapidly.

If these nucleoli were really immature because of the rapid cell division of cleavage, stopping cell division should allow them to mature into large prominent nucleoli. Fluorodeoxyuridine (FUdR), a compound that stops DNA synthesis by inhibiting thymidylate synthetase (*6*), was added to eggs in the presence of uridine at five times the FUdR concentration. Even at $10^{-2}M$, FUdR had no effect on cleavage until the 16-cell stage was reached. At this stage cell division was stopped by 10^{-2} to $10^{-3}M$ FUdR. As the concentration was lowered below $10^{-3}M$, cell division proceeded for longer periods beyond the 16-cell stage before stopping. At all concentrations of inhibitor, addition of thymidine at five times the FUdR concentration completely prevented the inhibition of cell division.

The nucleoli in cells treated with FUdR increased in size and density for about 2 hours after cell division stopped (Fig. 3, e and f). In many cases the fusion of the initial nucleolar blobs was inhibited, and eight to ten large nucleoli were formed. In some cases fusion was normal in FUdR, and a few large nucleoli resulted when cell division stopped. These results support the conclusion that the apparently atypical, multiple nucleoli are initial stages in the normal development of nucleoli that appear in all cells because the nucleoli do not have time to develop beyond these stages in the rapidly dividing cells of early embryos.

Our biochemical and cytological data indicate that rRNA synthesis is not repressed but only obscured by DNA-like RNA synthesis during cleavage of sea urchin embryos and that the "atypical" morphology of the nucleoli, usually attributed to decreased rRNA synthesis, is due to rapid cell division. We have reexamined the data from embryos (*1*) of other animals in which the results suggest that rRNA synthesis is repressed and find that the evidence available is entirely consistent with these new interpretations.

CHARLES P. EMERSON, JR.
TOM HUMPHREYS
Department of Biology,
University of California, San Diego,
La Jolla 92037

References and Notes

1. D. D. Brown and E. Littna, *J. Mol. Biol.* **8**, 145 (19(→ M. Nemer, *Proc. Nat. Acad. Sci. U.S.* **50**, 230 (1963); F. Wilt, *Develop. Biol.* **9**, 299 (19(→ V. R. Glisin and M. V. Glisin, *Proc. Nat. Acad. Sci. U.S.* **52**, 1548 (1964); D. G. Comb, S. Katz, R. Branda, C. Pinzino, *J. Mol. Biol.* **14**, 195 (1965); G. Giudice and V. Mutolo, *Biochim. Biophys. Acta* **138**, 276 (1967); G. Scinzo, A. M. Pirrone, V. Mutolo, G. Giudice, *ibid.* **199**, 435 (1970).
2. C. P. Emerson and T. Humphreys, *Develop. Biol.* **23**, 86 (1970).
3. G. Millonig, *Int. Congr. Electron Microscop. 6th* **2**, 345 (1966); S. Karasaki, *Exp. Cell Res.* **52**, 13 (19(→ F. J. Longo and E. Anderson, *J. Cell Biol.* **39**, 339 (1968); E. D. Hay and J. Gurdon, *J. Cell Sci.* **2**, 151 (1967).
4. C. P. Emerson and T. Humphreys, *Anal. Biochem.*, in press.
5. E. D. Hay, in *The Nucleus*, A. J. Dalton and F. Haguenau, Eds. (Academic Press, New York, 19(→ S. G. Phillips and D. M. Phillips, *J. Cell Biol.* **40**, 248 (1969).
6. C. Heidelberger, G. Kaldor, K. L. Mukherjee, P. B. Danneberg, *Cancer Res.* **20**, 903 (1960).
7. Supported by NIH grant HD-03480 and conducted with the assistance of R. Van Boxtel.

31 August 1970; revised 13 November 1970 ■

p-Nitrophenyl Phosphate Hydrolysis and Calcium Ion Transport in Fragmented Sarcoplasmic Reticulum

Abstract. *The calcium ion pump of fragmented sarcoplasmic reticulum can be coupled to hydrolysis of* p*-nitrophenyl phosphate, in the absence of added adenosine triphosphate. Comparison of the activities obtained with the two substrates suggests an analogous mechanism of transport. Independent of the substrate, a 2:1 ratio between calcium ion transport and substrate hydrolysis is displayed by the system, and an identical amount of work is required for ion transport against a given gradient. A phosphate ester appears necessary for substrate utilization in the pump mechanism, whereas the structure of the substrate determines the rates of activity and the affinity of the system for calcium ion.*

Vesicular fragments of sarcoplasmic membrane (SR) obtained from skeletal muscle homogenates rapidly accumulate Ca^{2+} in the presence of adenosine triphosphate (ATP). Simultaneous with Ca^{2+} uptake, a burst of ATP hydrolysis is also catalyzed by SR (*1*). Kinetic analysis of these activities indicates that, while a small amount of Ca^{2+} may bind to SR, most of the accumulated Ca^{2+} is transported inside the vesicles, forming a concentration gradient (*2*, *3*). The energy required by this pump is met by ATP hydrolysis (*4*). I now report experiments in which Ca^{2+} transport was coupled to hydrolysis of *p*-nitrophenyl phosphate (*p*-NPP). *p*-Nitrophenyl phosphatase activity has been observed in other membranes (*5*), but no direct relation to ion pumps was demonstrated.

Sarcoplasmic membrane was prepared by differential centrifugation of homogenized skeletal muscle (rabbit) (*1*). Sucrose (10 percent) was added to the homogenization and resuspension medium. To eliminate contaminations of myosin, the final SR suspensions were exposed for 1 hour to 0.6*M* KCl, recentrifuged, and resuspended. Accumulation of Ca^{2+} was measured by incubating SR in the presence of $^{45}CaCl_2$ in the reaction mixtures as required. After incubation, SR was removed by rapid filtration (Millipore HA0,45 μm); the residual radioactivity in the filtrate was determined by scintillation counting. In the experiments on *p*-NPP or ATP hydrolysis, incubations were interrupted by the addition of trichloroacetic acid (5 percent). After the denatured protein was removed by centrifugation, inorganic phosphate was determined by the method of Fiske and Subbarow (*6*). *p*-Nitrophenol was determined by direct spectrophotometric reading (400 nm) after addition of NaOH to the supernatants.

Curves of the rate of Ca^{2+} accumulation by SR, in the presence of *p*-NPP or ATP, are shown in Fig. 1. In spite of slower rates of uptake, relatively large amounts of Ca^{2+} are accumulated in the presence of *p*-NPP. In fact, the

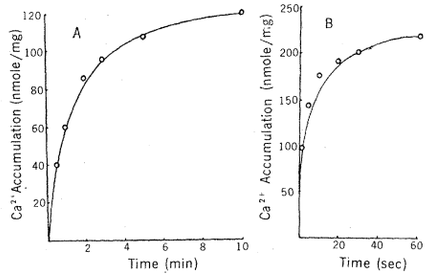

Fig. 1. Time curves of Ca^{2+} accumulation (nanomoles per milligram of protein) by SR. The reaction mixtures consisted of 16 m*M* tris-maleate (*p*H 6.8), 80 m*M* KCl, 0.1 m*M* EGTA, 0.12 m*M* $CaCl_2$, 10 m*M* $MgCl_2$; and either 10 m*M* *p*-NPP (A) or 5 m*M* ATP (B); and either 0.35 mg (A) or 0.175 mg (B) of SR protein per milliliter.